Interfacial characterization and thermal conductivity of diamond/Cu composites prepared by two HPHT techniques

Hui Chen · Chengchang Jia · Shangjie Li

Abstract With the aim of obtaining materials with high-thermal conductivities (TCs) for heat sink applications, diamond/Cu composites were produced via two different high-pressure-high-temperature (HPHT) techniques: powder metallurgy method (HPHT–PM) and infiltration method (HPHT–IM). The interfacial characteristics of composite materials are compared with respect to the sintering process and their effect on thermal properties is addressed. The HPHT–IM process is clearly more favorable than that of HPHT–PM and the obtained composites exhibited TCs as high as 717 W/mK for the former, but also as low as 200 W/mK for the latter. The advanced thermal property of HPHT–IM composites is attributed to a well-bonded interface layer with gradual and continuous element transition probably due to amorphous carbon detected by Raman spectra. EDS analysis indicate selective interfacial bonding between diamond {100} faces and Cu. Diamond skeleton with connected particles have been observed in this case, also resulting in enhanced interfacial bonding and thermal properties. The HPHT–PM composites with isolated diamond particles feature visible macro interfacial debonding, leading to rather low TC less than that of pure Cu.

Introduction

In the semiconductor industry today, both the increasing extent of integration and the decreasing size of electronic chips have produced a significant increase in power density, and the traditional heat sink materials are no longer sufficient to fulfill the requirements of heat removal of the most recent power electronic devices [1]. Accordingly, exploring thermal management materials with high-thermal conductivity (TC) to effectively dissipate heat becomes a very important issue for high-performance electronic packing materials, especially those used in state-of-the-art technology, such as laser diodes and microprocessors in laptops.

Owing to the excellent TC (1000–2000 W/mK), diamond-based composites such as those based on Cu, Al, Ag, and their alloys have attracted a worldwide attention of research and development activity in electronic packing materials with high TC [2–5]. Among them, diamond-reinforced Cu matrix (diamond/Cu) composites have received the most attention and have been considered to be the next generation of thermal management materials [6–11]. There are three points for developing composite materials with high-thermal conductivity: (1) Good wettability and interfacial bonding between diamond and matrix, which determines what extent the high-thermal conductivity of diamonds can be explored. (2) Volume fraction of diamond reinforcements as large as possible. (3) Diamond skeleton formation which can provide effective channels for heat conduction.

The expected diamond-Cu composite TC value is 400–1000 W/mK according to composite rule. But Cu is known to be naturally non-wetting with diamond. The crucial challenge of diamond-Cu composite fabrication is to establish a well-bonded interface until now, the carbide-forming metals B, Si, Ti, Cr, W are usually used to establish chemical interactions to force Cu to wet diamond [12], which would lead to a transition of the diamond/matrix from weak to strong bonding and in turn result in a great enhancement of composite thermal properties. The

H. Chen (✉) · C. Jia
School of Materials Science and Engineering, University of Science and Technology Beijing, Beijing 100083, China
e-mail: chenhui.ustb@gmail.com

S. Li
Shenzhen Haimingrun Industrial Co. Ltd, Shenzhen, China

most impressive progress in fabricating composites with a high TC by infiltrating Cu into diamond was announced in Refs. [13, 14]. The composite TC with some active element addition by this infiltration method was reported to reach 700 W/mK in Ref. [13]. But the thickness and microstructure of the interface products must be strictly controlled.

On the other hand, high-pressure-high-temperature (HPHT) sintering technique [3, 8, 15–18] have been recently applied favorably to make dense diamond/Cu composites. As early as 2004, Yoshida and Morigami first produced diamond/Cu composites via HPHT technique and investigated the effect of diamond particle size and volume fraction on TC and CTE of composites [3]. Then Kidalov et al. [7, 8] have made more work on HPHT sintering diamond/Cu composites, obtaining highest TC of even exceeding 900 W/mK at 8 GPa, a largely further TC enhancement than that obtained by infiltration method. Because sintering at pressures over 5–6 GPa and temperatures above 1600 K can lead to formation of a robust diamond skeleton composed of a cluster of connected particles, the diamond skeleton can more easily form path for heat flow through the composite, which is not provided by the same amount of isolated particles. But this can only be realized under very high-pressure and high-temperature which propose high requirements on equipment and limit the size and the complexity of accessible shape in thermal management components.

In this study, we provide a practical way to combine traditional HPHT and infiltration technique to prepare diamond/Cu composites with advanced thermal properties, namely high-pressure-high-temperature–infiltration method (HPHT–IM). For comparison, composites by a traditional high-pressure-high-temperature-powder-metallurgy method (HPHT–PM) have also been prepared. The microstructure and interfacial bonding between Cu and diamond in HPHT–IM and HPHT–PM composites were investigated with respect to its microstructure and interfacial element line scanning, fracture surface, and energy dispersive spectrum (EDS), paired with an analysis of the consolidation mechanism and the carbon state of diamond particle. Finally, the TCs of the composites were analyzed both theoretically and experimentally related to the differences in their interfacial microstructure.

Experimental

Materials and composites preparation

Synthetic available diamond powders (MBD-4 type) of the following grades were used as reinforcements in experiments in microns (mesh): 50/60 (286/238), 180/212 (79/67),

500/600 (28/23), provided by Shenzhen Haimingrun Industrial Co. Ltd. Both the pure bulk Cu and Cu powders (−500 mesh) have a 99.9% purity, supplied by research center for nonferrous metal composites in China.

Composites were fabricated by HPHT–PM and HPHT–IM technology, respectively. For the HPHT–PM method, Cu powders were mechanically mixed with various size diamond particles of 60% volume fraction for about 8 h and then put into a special cup. The enclosed cup was first subjected to vacuum heat treatment at 823 K about 2 h and then assembled into a pyrophillite mold. The main purpose for this is to prevent oxidation during HPHT sintering process, which is benefit to diamond particle sintering. Then the assembled system was consolidated at 5.3 GPa and 1473 K for 10 min in a cubic-pressing machine. Subsequently, the compact surfaces obtained were polished for analysis.

In the HPHT–IM process, diamond single crystals were tap-packed in the same special cup and an ingot of the metal was placed on top. This system was also assembled in a pyrophillite mold and received the same heat treatment as in HPHT–PM processing. Infiltration was also performed in the cubic-pressing machine at 5.3 GPa and 1473 K for 10 min. Then the samples were cut from as-sintered composites to remove extra metal.

Noting that PM is a powder metallurgy process, in which diamond and Cu powders were mixed together uniformly before sintering; while IM is an infiltration (penetration) process, in which solid-Cu was put onto diamond powders. The diamond volume fraction can be controlled in HPHT–PM process, but too high-diamond fraction can induce sintering failure (above 60% in this case) due to pressure loss discussed later in this article. For HPHT–IM method, pure Cu metal was used as a binder of diamonds and much higher diamond fraction can be obtained in this case. The binder-to-diamond volume radio was experimentally selected under the condition that the binders were completely infiltrated into the diamond powders. So the volume fraction of Cu binder can be estimated to be 10–20% with various diamond sizes under the assumption of complete densification. All the samples were cut by laser cutting machine from as-sintered composites to disk-shaped with a diameter of 10 mm and a thickness of 3 mm.

Characterization

The original cylindrical samples were mechanically broken into pieces to allow for the investigation of the fracture surfaces. The surface microstructure and fractography of composites were examined on a LEO1450 scanning electron microscopy (SEM). Interfacial atomic composition was analyzed by energy dispersive X-rays spectrometry

(EDS) attached to the SEM. Raman spectra were acquired at 532 nm using a power of 1 mW to investigate carbon state. The bulk density (ρ) of all the samples was measured based on Archimedes' principle. The theoretical densities of pure Cu (8.96 g/cm^3) and diamond (3.52 g/cm^3) were used to calculate the relative density of composites. Thermal diffusivity (α) of all the composites at room temperature were evaluated using a laser flash technique on LFA 447 Nanoflash equipment from Netzsch.Lab. The heat capacity (C_p) of the specimens was measured using a differential scanning calorimeter with single crystal alumina as reference under argon gas. The uncertainty in the thermal measurements is ±2%. Thermal conductivity (K) was then calculated by $K = \alpha \cdot C_p \cdot \rho$. A detailed description of the measurement technique was summarized elsewhere [19]. Thermal physical properties at room temperature of all the samples are given in Table 1.

Results

Microstructure and interfacial atomic composition

The surface microstructure of all the composites with various particle sizes by the two HPHT techniques has been investigated, as shown in Fig. 1. As seen, there are no visible pores in any of the consolidated composites, indicating that dense samples can be well prepared by the HPHT technique. And diamond particles are dispersed homogeneously in the matrix even for large particle size (500/600 μm), as illustrated in Fig. 1c, f. As such, the distance between particles decreases as the volume fraction of diamond particles increases from 60 to 85%.

Figure 1b, c shows the high-magnification SEM of HPHT–PM samples. Here, debonding between the metal-matrix and the diamond particles occurs and macro-cracks at the diamond-Cu interface are visible. The same defects, however, cannot be observed in HPHT–IM samples (cf. the high-magnification image of Fig. 1e). Figure 1f shows that

the diamond particles are not only tightly bonded to the matrix, but also connected with each other by creating bridges. Also, diamond particles did brake and were damaged to some extent under such high pressure (5–6 GPa) in both HPHT–PM and HPHT–IM composites, especially in large size as seen in Fig. 1c, f.

The interface chemistry distribution of samples B and E in high magnification of Fig. 1b, e has been analyzed by EDX line scanning, presented in Fig. 2. It can be clearly seen that the intensity of the carbon signal decreases slightly from diamond to Cu with gradually increasing Cu signal at the interface of HPHT–IM sample (Fig. 2b). For HPHT–PM composite, however, the carbon signal sharply decreases at the diamond-Cu interface and correspondingly the Cu signal sharply increases (Fig. 2a). So the element distribution at diamond-Cu interface is gradual and continuous in the IM case but sharp and not continuous in the PM case. Although the absolute values of X-ray intensity across interphase boundaries may suffer from bias due to topography contrast, the observation of element distribution at diamond-Cu interface is meaningful. Furthermore, the diamond skeleton has been identified (Fig. 2c), indicating a strong diamond–diamond bonding contact in HPHT–IM composites.

Fracture surfaces and EDS test

Figure 3 presents fracture surfaces of composites with diamond particle of the same micro size (500/600 μm). The comparison between Fig. 3a, b gives evidence that different topographies and interfacial morphologies occur. In the typical case of HPHT–PM composites, most of the diamonds maintains their original morphology and are bare on the fracture surfaces with large Cu pits remaining. This indicates that the interface fracture strength between diamonds and matrix is much lower than that of both diamond and matrix. The interfacial debonding indicated by arrows in Fig. 3a suggests weak interfacial bonding between the diamond and Cu. A good interfacial

Table 1 Thermal diffusivity (α), thermal capacity (C_p), Thermal conductivity (K), experimental density (ρ), and relative density (RD) with various diamond particle sizes (D) for all composite specimens

Process	Sample	D (μm)	α (mm^2 s^{-1})	C_p (J g^{-1} K^{-1})	K (W m^{-1} K^{-1})	ρ (Kg m^{-1})	RD (%)
HPHT–PM	A	50–60	71.2	0.481	190.8	5.57	97.8
	B	180–212	80.6	0.459	207.5	5.61	98.5
	C	500–600	87.6	0.453	224.2	5.65	99.1
HPHT–IM	D	50–60	265.3	0.501	554.3	4.17	>99
	E	180–212	347.6	0.496	682.7	3.96	>99
	F	500–600	370.5	0.495	717.1	3.91	>99

Fig. 1 SEM images of diamond/Cu composites in various diamond particle sizes (μm) in different processing **a** HPHT–PM 50/60, **b** HPHT–PM 180/212, **c** HPHT–PM 500/600, **d** HPHT–IM 50/60, **e** HPHT–IM 180/212, **f** HPHT–IM 500/600
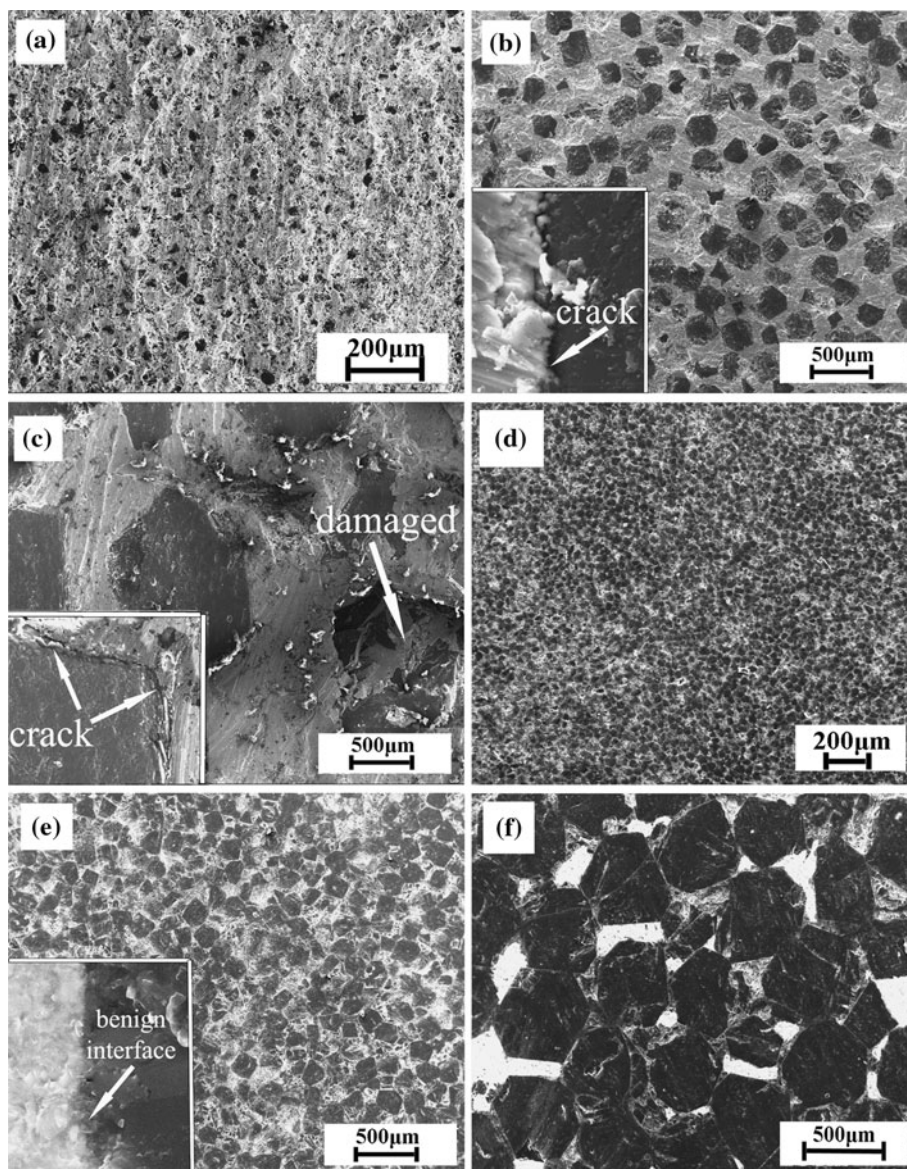

adhesion, by contrast, can be observed for HPHT–IM samples (Fig. 3b), in which most diamonds are tightly embedded into the Cu matrix and some diamonds are even ruptured. A, B, and C in Fig. 3b represents cleavage diamond face, Cu pits and drawn diamond from matrix, respectively. It is worth noting that few diamonds were pulled-out and selectively adhered to the matrix on diamond {100} faces. Furthermore, the pulled-out diamond surfaces of two HPHT samples were tested by EDS element analysis, shown in Fig. 4. As illustrated, all the faces of the pulled-out diamond particles sintered by HPHT–PM are smooth and only detected carbon signal. In contrast, the {100} faces of the pulled-out diamond sintered by HPHT–IM were rough and detected both C and Cu signal. But the {111} surfaces were smooth and adhered no matrix.

Raman spectra

Micro-Raman spectroscopy, shown in Fig. 5, was used to detect different areas of both HPHT–PM and HPHT–IM composites to investigate the microstructure and carbon state of diamond particles subjected to the HPHT sintering process. Figure 5a shows the micro-Raman spectra of PM sample detected in the diamond particle and nearby the interface between diamond and Cu, respectively. Both the spectra exhibit only a sharp peak near 1332 cm^{-1}, which is attributed to crystalline diamond. The micro-Raman spectrum of IM sample, shown in Fig. 5b, is obviously quite different. Both spectra of diamond particle and interface display not only a sharp peak near 1332 cm^{-1} but also a broad peak around 1400–1500 cm^{-1}, which are characteristic for diamond

Fig. 2 EDS interfacial line scanning images in diamond/Cu composites **a** HPHT–PM from matrix to diamond, **b** HPHT–IM from matrix to diamond, **c** HPHT–IM between diamond grains
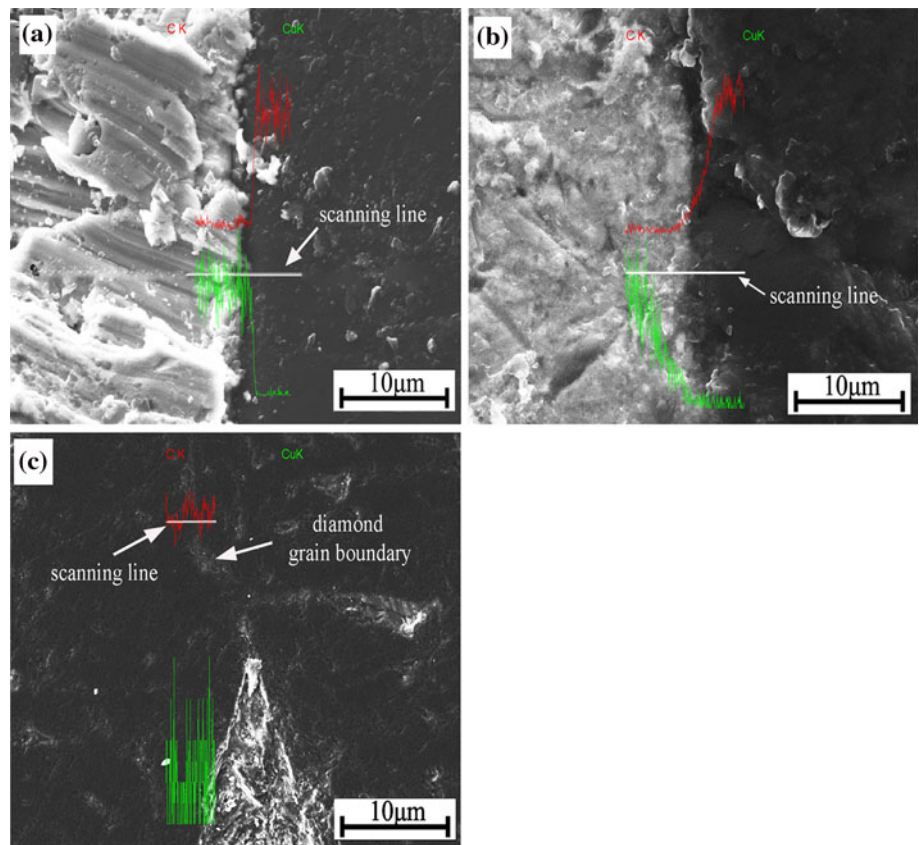
Fig. 3 Fracture surface micrographs of diamond/Cu composites in 500/600 μm prepared by **a** HPHT–PM, **b** HPHT–IM
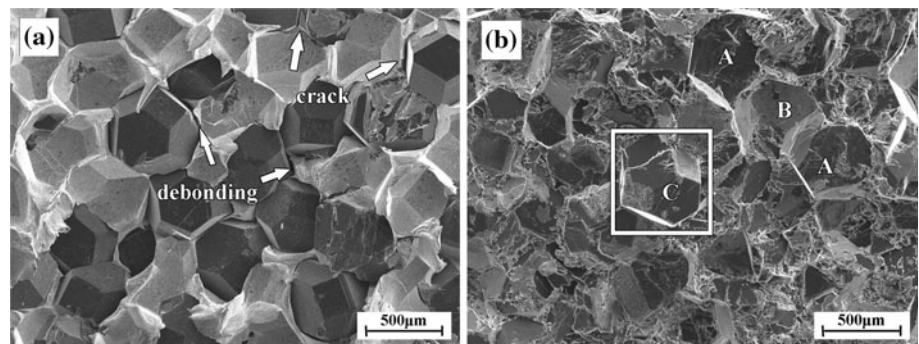
and amorphous carbon, respectively. In addition, the graphite peak, showing one single line at 1575 cm^{-1}, does not appear at all, indicating no graphitization in all the samples.

TCs of the composites

Table 1 shows the thermal physical properties of all the samples with various diamond sizes prepared by HPHT–PM and HPHT–IM, respectively. As seen, TCs of the HPHT–IM samples were found to be significantly higher than those of the HPHT–PM samples, which even have a lower TC than that of pure Cu. Also composite TCs increase with increasing diamond size. But TCs of HPHT–PM samples are more insensitive to the diamond particle size than those of HPHT–IM samples.

Discussion

The diamond/Cu composites produced by two HPHT techniques exhibit significant differences in their interfacial microstructures, carbon state of diamond particles and TCs, depending on the production process and consolidation mechanism.

In the following, first the differences of the interface microstructures and carbon state of diamond observed in two HPHT samples will be discussed. Then, the effects of these differences on the composite TCs will be addressed.

Fig. 4 EDS element analysis on diamond {100} faces of **a** HPHT–PM sample, **b** HPHT–IM sample
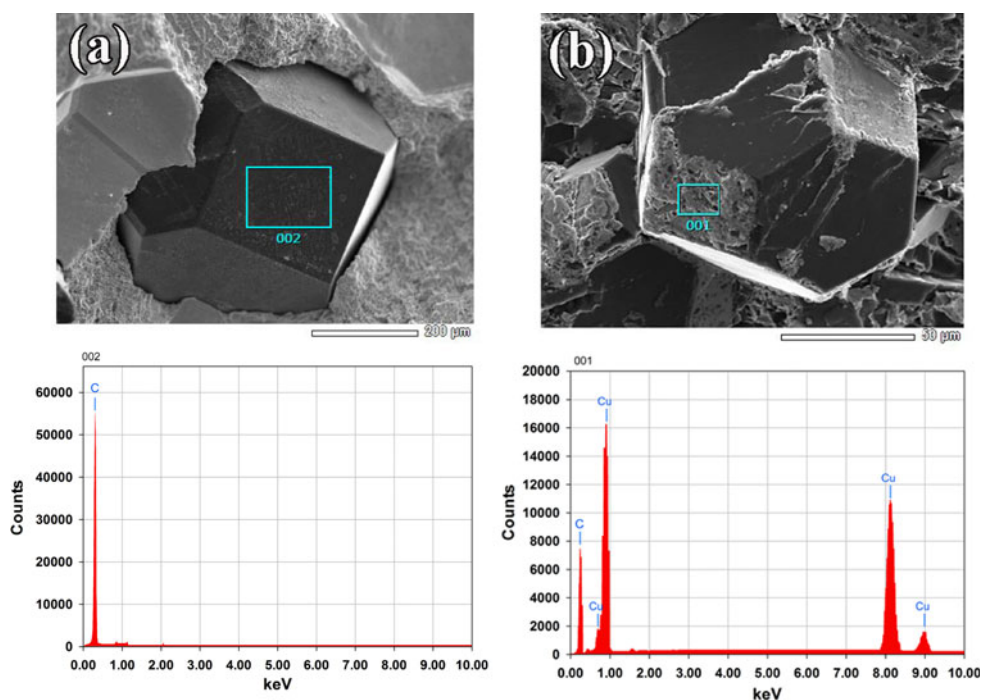
Relationship between interface microstructure and carbon state of diamond

It can be found from the SEM results that the interfacial bonding between diamond and Cu in HPHT–IM case is much stronger than that in HPHT–PM case. The observation from X-ray line scanning analysis suggests that good adherence of Cu to diamond in the HPHT–IM composites is seemingly attributed to a interfacial layer with gradual and continuous element distribution, which can be seen as benign interface with no macro interfacial debonding. In contrast, the absence of such interface layer for the HPHT–PM composites is thought to be a main reason for the low interfacial adhesion strength.

The improvement of interfacial bonding is likely due to the presence of amorphous C. As of date, Raman spectroscopy is the best way to obtain the detailed bonding structure of carbon [21]. First, we can confirm that no graphite phase exists in both HPHT–PM and HPHT–IM samples from Raman analysis, indicating that the graphitization of diamond could be well suppressed to a great extent in the diamond/Cu composite materials via the present composite fabrication route. This result is quite in accordance with the conclusion in Ref. [20]. As seen in Fig. 5, amorphous carbon only existed in HPHT–IM composites both in diamond particle and near the interface. The atomic bonding structure of the observed amorphous carbon is considered to be sp^2/sp^3 co-configuration (mainly sp^2 configuration) according to other researches [22, 23]. Amorphous carbon yields disordered structure which is consist of dissociative carbon segments and pieces with

broken and dangling bonds and/or clusters of fused sixfold rings [24]. Such disordered structure can make diamond surface rough and increase the specific surface area, thus widening the interface layer bonded to Cu. It is reasonable to assume that the wide interface layer with gradual and continuous element distribution is possible due to the existence of this kind of amorphous carbon.
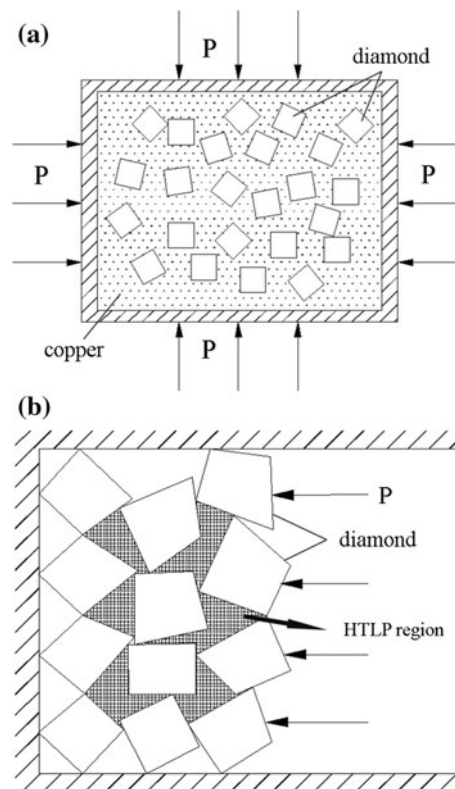
Furthermore, it is also worth noting that the enhancement of the diamond-Cu interfacial bonding only occurred on diamond {100} faces in HPHT–IM samples. This can be rationalized by carbon atoms bonded to the bulk by three C–C bonds on {111} diamond surfaces, while carbon atoms on {100} diamond surfaces are only bonded twofold to the bulk. Hence, the carbon transition from diamond to amorphous on {100} faces is expected to be easier than {111} ones. A similar selective interfacial bonding in diamond-Al composites was reported in Ref. [28].

The large discrepancy of interfacial structure and carbon state of diamond surface between HPHT–PM and HPHT–IM composites is strongly related to the difference between HPHT–PM and HPHT–IM techniques. As seen in Fig. 6b, diamond particles were tap-packed together with Cu slice above them. When pressure is applied, diamond particles with sharp corners push each other and the large pressure stress distributes only on the contact points of diamond crystallite. As a result, the intact diamond surfaces in a condition of high-temperature-low-pressure (HTLP) are prone to amorphizing first [25, 29] and, in this case, the carbon on the surface of diamond is respected to transform into amorphous carbon. Noting that, in IM samples, some diamond particles are ruptured and damaged under such high
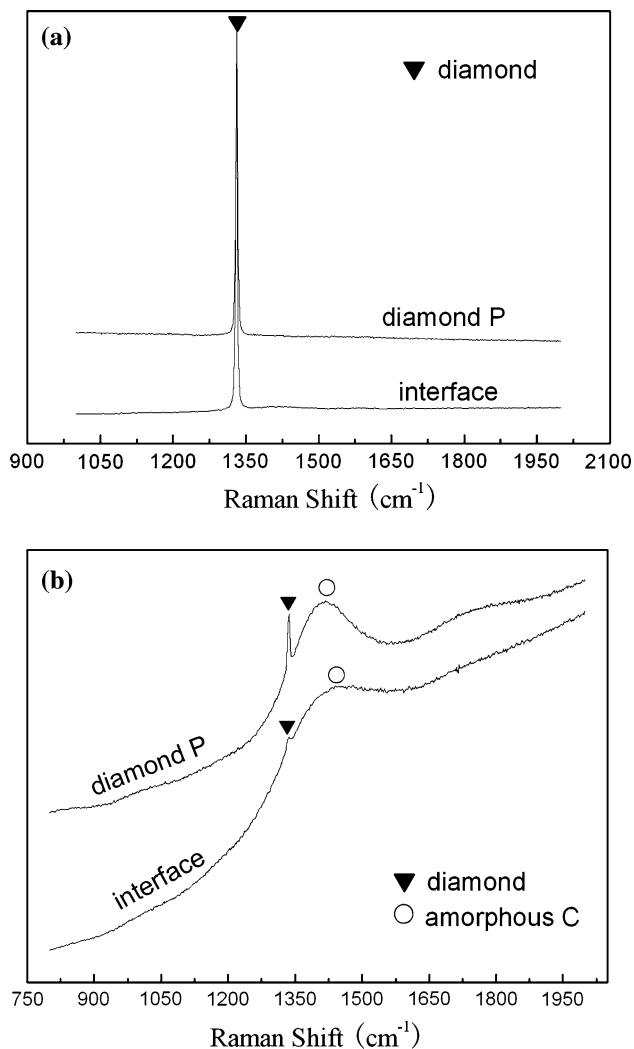
Fig. 5 Raman Spectra of diamond/Cu composites both in diamond particle and near the diamond-Cu interface **a** for HPHT–PM, **b** for HPHT–IM

Fig. 6 Schematic illustration drawings of pressure distribution on diamond surface fabricating via **a** HPHT–PM, **b** HPHT–IM. The polyhedral-reinforced diamond particles are equivalent to quadrilateral ones and the shaded part represents high-temperature and low-pressure region (HTLP region)

to bind diamond particles into compacts, thus reducing the composite thermal conductivity. Hence, it can be assumed that the loading method of materials and sintering mechanism are contributed to enhancement of interfacial bonding and thermal properties of composites.

Relationship between interface microstructure and TC

Interfaces in composites are known to be crucial to TC, as they determine to which extent the properties of a highly conductive reinforcement phase such as diamond can be exploited. In order to understand the TC behavior of composites, it is important to compare the experimental results with theoretical predictions. The Maxwell approximation-based Hasselman and Johnson (H–J) model [26] is frequently applied to estimate the TC of MMCs with particle reinforcements in which the Kapitza interfacial thermal resistance and size effect of the inclusions are considered:

pressure. So the grain size of diamond particles is indeed smaller than the raw materials. This is unfavorable for the thermal conductive performance of diamond but favorable for compact densification and diamond skeleton formation. On the other hand, in the HPHT–PM process, diamond particles and Cu powders are well mixed, as illustrated in Fig. 6a. So the pressure loaded on each diamond particle is uniform. Actually, the pressure in the cavity of cubic machine is greatly lost when Cu melted, resulting in macro pores and cracks (poor interfacial bonding) in composites and lower relative density than IM samples. So a small amount of metal-matrix (less than 40% volume fraction) fails

$$K_c = K_m \left\{ \frac{2 \left[(K_p/K_m) - (K_p/ah_c) - 1 \right] V_p + (K_p/K_m) + (2K_p/ah_c) + 2}{\left[1 - (K_p/K_m) + (K_p/ah_c) \right] V_p + (K_p/K_m) + (2K_p/ah_c) + 2} \right\}$$

where K is the TC, the subscripts c, m, and p refer to composite, matrix and reinforced particles, respectively. a and V_p are the average radius and the volume fraction of reinforced particles, respectively. h_c is the value of the intrinsic interfacial thermal conductance and its reciprocal is the interfacial thermal resistance (ITR). In this calculation, K_m, K_p are taken to be 400 and 1000 W/mK, as well as the h_c is 4.87×10^7 W/m^{2}K (corresponding ITR is 2.05×10^{-8} m^{2}K/W) obtained by a simple Debye model in terms of the acoustic mismatch theory [19]. Substituting these parameters into Eq. 1, the comparison between our experiments and theoretical calculations are shown in Fig. 7, in which the dashes represent the TC of pure Cu.

As seen, the TCs of HPHT–IM composites show much better agreement with predictions than those of HPHT–PM composites where a large discrepancy can be found. The HPHT–PM composites were found to have TCs even less than that of pure Cu. This implies that the high TC of the

diamond particles does not contribute to the composite TC in this case due to rather poor interfacial bonding induced by macro defects such as pores and cracks (Fig. 1b, c) at the diamond/Cu interfaces. In contrast, the IM samples exhibit well-bonded interfaces with gradual element distribution and no macro defects. In addition, diamond skeleton formation largely enhance composite TC because the particle grain boundary resistance is lower than that of the particle–matrix thermal resistance by one order of magnitude [27]. Although H–J model is no longer adapted in this case, we can also conclude that theoretical expected TC can be reached by IM samples.

As seen in Fig. 7, the TC of HPHT–IM composite has been apparently enhanced with the diamond particle size increasing, while the TCs of all the HPHT–PM composites are approximately the same. We further confirm that the influence of poor interfacial adhesion is prominent over other effects that might be introduced, so the increased particle size fails to contribute to composite TC improvement in this case.

Conclusions

Diamond/Cu composites were fabricated via two different HPHT techniques: HPHT–PM and HPHT–IM and their interface microstructures and thermal conductivities have been evaluated, respectively. It is found that the pressure employed during HPHT–IM, notably distributes only on the contact points of diamond crystallite and the HTLP region among them results in the formation of amorphous carbon at the diamond particle surface. The strong interfacial bonding of HPHT–IM composites is attributed to the gradual element transition interface layer with no macro defection between amorphous carbon and liquid Cu. And the enhancement of interfacial bonding is preference on diamond {100} faces. Diamond skeleton with connected particles has also been found in this case. Both result in strong interfacial bonding and an improved bulk TC for HPHT–IM composites as high as 717 W/mK.

In contrast, the HPHT–PM composites with isolated diamond particles within Cu matrix feature visible macro interfacial debonding between two phases, resulting in weak interfacial bonding and rather lower TC than that of pure Cu. The poor interfacial bonding due to pressure loss during PM process limits the diamond volume fraction to no more than 60%. The present experimental HPHT–IM technique first provides a practical way to achieve super-density and rather high TC even under the "mild HPHT condition" [15] without any element addition [12], and therefore addresses the problem of diamond-Cu poor wettability.
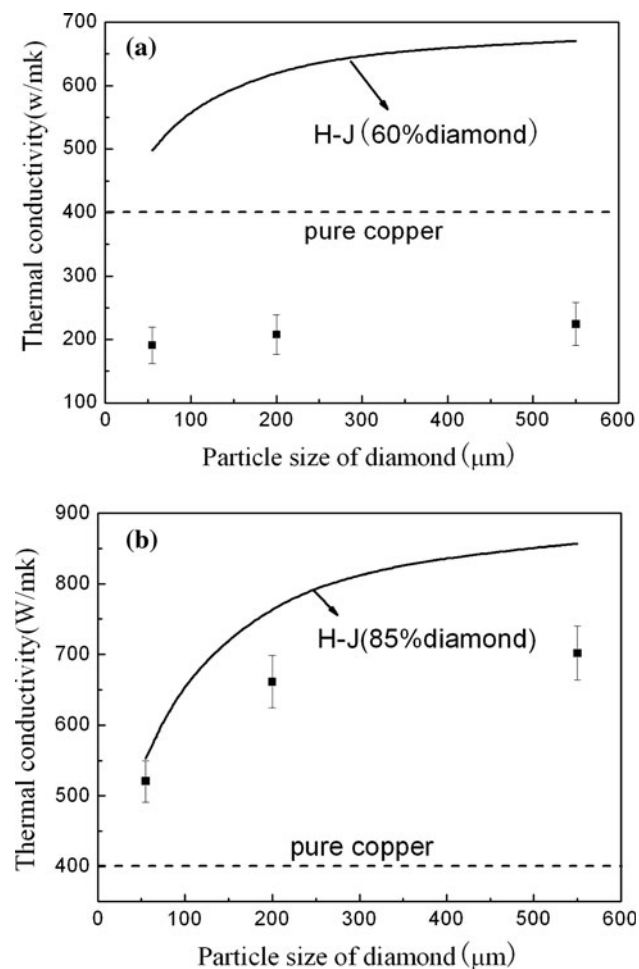
Fig. 7 Comparisons of the H–J predictions and the experiments for the TC of diamond/Cu composites as a function of the particle size of diamond prepared by **a** HPHT–PM, **b** HPHT–IM

References

1. Zweben C (2006) Power Electron Technol 40:40
2. Hanada K, Matsuzaki K, Sano T (2004) J Mater Proc Technol 153–154:514
3. Yoshida K, Morigami H (2004) Microelectron Reliab 44:303
4. Molina J-M, Rhême M, Carron J, Weber L (2008) Scr Mater 58:393
5. Tavangar R, Molina JM, Weber L (2007) Scr Mater 56:357
6. Sun Q, Inal OT (1996) Mater Sci Eng B 41:261
7. Kidalov SV, Shakhov FM, Vul AY (2007) Diam Relat Mater 16:2063
8. Kidalov SV, Shakhov FM, Vul AY (2008) Diam Relat Mater 17:844
9. Schubert T, Ciupiński Ł, Zieliński W, Michalski A, Weißgärber T, Kieback B (2008) Scr Mater 58:263
10. Schubert T, Trindade B, Weißgärber T, Kieback B (2008) Mater Sci Eng A 475:39
11. Chu K, Jia CC, Liang XB, Chen H, Gao WJ, Guo H (2009) Mater Des 30:4311
12. Ferralis N (2010) J Mater Sci 45:5135. doi:10.1007/s10853-010-4673-3
13. Weber L, Tavangar R (2007) Scr Mater 57:988
14. Weber L, Tavangar R (2009) Adv Mater Res 59:111
15. Ekimov EA, Suetin NV, Popovich AF, Ralchenko VG (2008) Diam Relat Mater 17:838
16. Ekimov EA, Suetin NV, Popovich AF, Ralchenko VG, Gromnitskaya EL, Modenov VP (2008) Inorg Mater 44:224
17. Nauyoks S, Wieligor M, Zerda TW, Balogh L, Ungar T, Stephens P (2009) Compos Part A 40:566
18. de Azevedo MG, Potemkin A, Skury ALD (2001) Diam Relat Mater 10:1607
19. Chu K, Liu ZF, Jia CC, Chen H, Liang XB, Gao WJ, Tian WH, Guo H (2009) J Alloy Compd 490:453
20. Shao WZ, Ivanov VV, Zhen L, Cui YS, Wang Y (2003) Mater Lett 58:146
21. Wang Y, Alsmeyer DC, McCreery RL (1990) Chem Mater 2:557
22. Robertson J (2002) Mater Sci Eng R 37129-281
23. Ferrari AC, Robertson (2001) Phys Rev B 64:075414
24. Robertson J, O'Reilly EP (1987) Phys Rev B 35:2946
25. Sumiya H, Yusa H, Inoue T, Ofuji H, Irifune T (2006) High Press Res 26:63
26. Hasselman DPH, Johnson LF (1987) J Compos Mater 21:508
27. Chen H, Chu K, Jia CC, Liang XB, Guo H, Qu XH (2011) J Mater Sci Technol 27:713
28. Ruch PW, Beffort O, Kleiner S, Weber L, Uggowizer PJ (2006) Compos Sci Technol 66:2677
29. Scott PM, Nicholas M, Dewar B (1975) J Mater Sci 10:1833. doi:10.1007/BF00754470